ISSN (e): 2250 – 3005 || Volume, 14 || Issue, 3|| May. - June. – 2024 ||
International Journal of Computational Engineering Research (IJCER)

An Improved Accurate State of Charge Prediction of Lithium-ion Batteries Based on Long Short-Term Memory-Extended Kalman Filtering Algorithm

Emmanuel Appiah[1],ShunliWang[1,2] Chuan-yun Zou[1],Paul Takyi-Aninakwa[1], Bobobee Etse Dablu[1],Daniel-Ioan Store[2]

1. *School of Information Engineering, Southwest University of Science and Technology, Mianyang 621010, China;*
2. *Department of Energy Technology, Aalborg University, Pontoppidanstraede 111, 9220 Aalborg East, Denmark*

Abstract:
Accurate predictions of the state-of-charge (SOC) are very difficult since batteries have nonlinear characteristics and the electric vehicle (EV) application environment is complex, especially at low temperatures and low SoC. In lithium-ion batteries and other prediction research, it helps the long short-term memory (LSTM) network to produce a more accurate SOC estimation.This study examines how the working conditions for datasets used for training and testing affect the precision of SOC estimation using an LSTM network. An extended Kalman filter (EKF) is used to create hybrid models that iteratively denoise and maximize the accuracy of the final SOC predictions under three difficult operating situations based on the SOC calculated by the LSTM. These error results demonstrate the correctness and resilience of the suggested hybrid models, LSTM-EKF, in comparison to the data-driven approaches used in the model LSTM network. Both the estimation error result under the BBDST working condition and the maximum estimation error under the entire HPPC working condition are less than 0.03, indicating strong stability and robustness.

Keywords:*Lithium battery, state of charge prediction, long short-term memory, extended Kalman filter*

Date of Submission: 29-04-2024 Date of acceptance: 08-05-2024

I. Introduction

Due to their advantages over other batteries with various chemistries, such as higher energy density and longer lifespan, lithium-ion batteries are currently the most widely used battery in electronic gadgets (EGs) and electric vehicles (EVs)[1, 2].Longer driving ranges, quicker speeds, and more potent energy sources are all necessary for EV performance needs. Still unable to supply enough energy to propel EVs farther than gasoline in conventional cars. The precision of a lithium-ion battery's parameter detection is linked to both its safety and efficiency [3-5]. The battery management system (BMS) is designed to supervise and track the battery's data, such as current, voltage, and temperature, to ensure both the battery's safety and the power system's reliability. In these conditions, the BMS should be used to completely use the energy that EV batteries have to offer[6].

The accuracy of the state of charge (SOC) estimate is a key responsibility of the BMS and affects how well other BMS functions operate, including charging control[7], balancing control[8], thermal management[9], and safety management[10]. Since the nonlinear features and various working environments of EV batteries make correct SOC extremely difficult to achieve, the BMS needs a well-designed SOC estimate mechanism[11].Due to its minimal computation and reliable results, the ampere-hour (Ah) method was previously the most used approach for calculating the SOC in BMS when combined with beginning value adjustment via a look-up table[12].Nevertheless, the approach only accounts for accurate battery capacity, which is difficult to ascertain in practical applications[13]. Typically, capacity estimation methods require a particular, steady environment that is distinct from that of electric vehicles[14].

Certain techniques developed using the neural network methodology and machine learning will significantly increase the processing load on the BMS since they require large amounts of computation and training data. Furthermore, data-driven algorithms' accuracy is impacted by the quality of training samples[15, 16]. The model-based approach is ubiquitous, and the estimation accuracy is independent of historical data. The

integral technique is the basic SOC method in the conventional method, even though it has both initial and cumulative flaws[17, 18]. There has been minimal accuracy in the estimation[19].Although this corrective mechanism allows model-based SOC prediction algorithms to partially accept battery capacity error, it also requires a more accurate battery model.[20].

Data-driven estimation approaches have attracted more attention recently because of the developments in big data and artificial intelligence techniques. These methods often use machine learning algorithms to characterize SOC estimation based on historical monitoring data[21, 22]. Over the course of charging or discharging, these statistics typically include voltage, current, and other measurable data. In [23], utilized the least squares support vector machine to create an estimation model after extracting the aging features from the short-term charging profiles of lithium-ion batteries. In [24, 25], the relevance vector machine to map the nonlinear relationship between other parameters and the SOC estimate. Furthermore, several approaches to estimating the SOC of lithium-ion batteries have been documented in the literature. These include Gaussian Process Regression[26], Random Forest, and BP Neural Network (BPNN)[27].

As one of the most promising data-driven techniques for determining the state of charge (SOC) of batteries, long short-term memory (LSTM) neural networks have dominated deep learning algorithms due to their superiority in processing time series data [28]. In [29], proposed a novel technique for estimating the SOC of batteries using stacked LSTM and rapid charge data. Experiments were conducted to confirm the efficacy of this technique. In [30, 31], proposed a method for estimating system outage SOH that combines enhanced incremental capacity (ICA) with LSTM neural network. The experimental findings showed that the maximum error is limited. In[32], an LSTM-based approach for lithium-ion batteries was introduced. To predict the conditions of different types of batteries, transfer learning was employed. It's crucial to keep in mind that, despite LSTM's proven effectiveness in battery SOC prediction, there are still several outstanding problems[33]. For instance, the key model hyperparameters, including the quantity of neurons in each LSTM layer, have been pre-defined by the research's inventor.

Finding the hyper-parameters is typically difficult, and choosing these aspects largely depends on experience. The LSTM-based SOC estimation methodologies' estimation accuracy will be affected by the selection of hyperparameters. In situations where the filtering error and the prediction error are negligible, the EKF is utilized to accurately and instantly realize the SOC estimation. There are numerous ways to extend the Kalman filter to nonlinear systems using modified Kalman filtering, or KF. When first-order Taylor series expansion is utilized to linearize the nonlinear system, the EKF technique will inevitably ignore the high-order terms, leading to large linearization errors.

When the filtering error and the prediction error are minor, the EKF is utilized to correctly and in real time perform the SOC estimation. A network structure is suggested by the LSTM-EKF model to deal with the problem of gradient explosion or disappearance in the LSTM. The classic LSTM's state unit is replaced with the cyclic unit structure of the LSTM-EKF model. The accuracy of the LSTM-EKF-based SOC calculation is dependent on the accuracy of the battery model, and the primary reason of the divergence of LSTM-EKF is the linearization mistake for removing high-order terms. The hybrid models that are produced by feeding the LSTM-estimated SOC into an EKF under three difficult operating conditions consistently reduce noise and enhance the precision of the final SOC estimations.These error results show that the proposed hybrid models, LSTM-EKF, are resilient and correct when compared to data-driven approaches of the model LSTM network. The accuracy of SOC estimate using an LSTM network is investigated in this study in relation to the working conditions utilized for training and testing datasets. As a data optimizer, a pertinent attention mechanism is incorporated into the LSTM network. In order to create a hybrid model that iteratively denoises and optimizes the accuracy of the final SOC estimations of HPPC, BBDST, and DST operating conditions, the SOC predicted by the LSTM is fed into an EKF.

The rest of the paper is structured as follows: The methodology and the theoretical analysisof the Long Short-Term Memory Network and Extended Kalman Filtering Algorithm are shown in Section 2. In Section 3, the battery experiment platform and the outcomes and discussions of the experiment are presented. In Section 4, finally, wrap up the paper.

II. Mathematical Analysis

2.1 Neural Network for Battery Modeling

In this section, the structure and the training algorithm of long short-term memory (LSTM) are first introduced as preparation and then its application to the battery modeling will be described in detail.

2.1.2 Long Short-Term Memory

To solve the problem of gradient explosion or disappearance in the LSTM network structure of the LSTM-EKF model is proposed and the state unit of the classical LSTM is replaced by the cyclic unit structure of the LSTM-EKF model.The extension of the feedforward neural network (FNN) is the recurrent neural network (RNN). The

running process of lithium-ion batteries, through the capacity test, charge and discharge experiment, and the experimental data analysis of 4.2V/40Ah ternary lithium-ion batteries. The self-discharge rate of lithium-ion batteries has been reduced greatly due to the improvement of the manufacturing process. The structure of LSTM and EKF for the SOC estimation is presented in Figure 1.

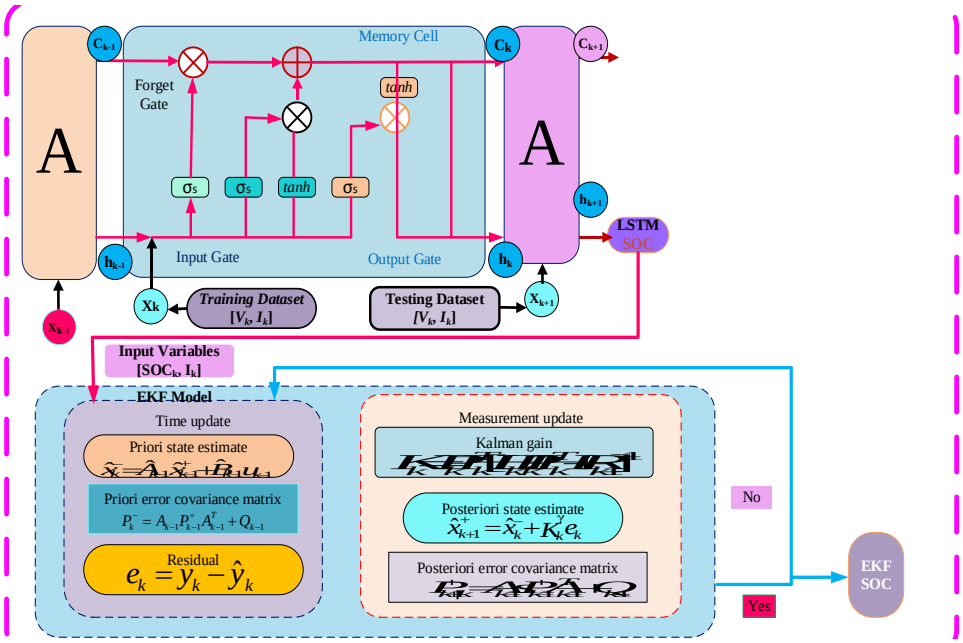

Figure 1: The Structure of LSTM and EKF for the SOC Estimation

σ is the sigmoid layer that helps the LSTM network to either discard or update information by closely directing it to 0 and 1, respectively. the tanh is the hyperbolic tangent function that controls the information flowing through the network between -1 and 1 to avoid the fading effect.

$$\hat{X}_k^+ = \hat{X}_k^- + K_k^{\Upsilon} * (y_k - \hat{y}) \quad (1)$$

$$P_{k+1/k}^+ = A_{k-1}(SP_{k+1/k}^+)A_{k-1}^T + Q_{k-1} \quad (2)$$

Equations (1) and (2),ϒ is the weighting parameters, which are tuned within 2<ϒ>4, to denoise the estimated SOC and make it more adaptable to the actual SOC of the battery system. Also, Ssis the fading factor tuned within a range of 0.80<s<1.

The three gates of the LSTM model are the forget gate f_t, input gate i_t, and output gate o_t, to protect and control the memory cell C_t. the mathematical expressions and working principle for the gates. The forget gate controls the degree of forgetting of historical information as shown in Equation (3).

$$f_t = \sigma_s * (W_f * [x_t, \square_{t-1}] + b_f) \quad (3)$$

The input gate controls the memory level of the current input information as shown in Equation (4).

$$\begin{cases} i_t = \sigma_s * (W_i * [x_t, \square_{t-1}] + b_i) \\ \tilde{C}_t = tan\square * (W_c * [x_t, \square_{t-1}] + b_c) \end{cases} \quad (4)$$

The output gate controls the extent to which the current internal state. An output of 1 means that information passes and 0 means that the threshold is closed so that no information can pass are shown in Equations (5) and (6).

$$C_t = f_t * C_{t-t} + i_t * \tilde{C}_t \quad (5)$$

$$\begin{cases} o_t = \sigma_s * (W_i * [x_t, \square_{t-1}] + b_i) \\ \tilde{C}_t = tan\square * (W_c * [x_t, \square_{t-1}] + b_c) \end{cases} \quad (6)$$

σ_s is the sigmoid layer, which helps the LSTM network to either discard or update information by closely directing it to 0 and 1, respectively. The *tanh* is the hyperbolic tangent function that controls the information flowing through the network between –1 and 1 to avoid fading. Each gate in the network has a weight W_f, W_i, W_c, and W_o associated with the forget gate, input gate, memory cell, and output gate, respectively. Also, each gate of the network possesses a bias b_f, b_i, b_c, and b_o vector by the forget gate, input gate, memory cell, and output gate, respectively, to enhance the flexibility of the network to adapt to the training data for accurate SOC.The attention mechanism of humans to select the relevant inherent features from a piece of information,

this study employs the attention mechanism as a relevant data optimizer due to its working mechanism. The attention mechanism for the n-dimensional feature sequence $x_t n$ in the input data sequence x_t is established based on the hidden state h_{t-1} and the cell state of the encoder layer's output unit o_t at the previous time step, as expressed in Equations (7), (8), (9), (10), and (11):

First stage attention-weighted:

$$\tilde{x}_t = (e_t^1 x_t^1, e_t^2 x_t^2, \ldots, e_t^n x_t^n)^T \tag{7}$$

Encoder layer:

$$\square_t = f_1 * (\square_{t-1}, \tilde{x}_t) \tag{8}$$

Weighted vector calculation:

$$m_t = tan\square * (W_d * [\square_t, s_{t-1}] + b_d) \tag{9}$$

Attention probability:

$$\beta t = \frac{exp(m_t^n)}{\sum_{t=1}^{n} exp(m_t^n)} \tag{10}$$

Weighted vector calculation:

$$x_{t-1} = \sum_{t=1}^{n} \beta_t \square_t \tag{11}$$

2.1.3 Extended Kalman Filter Algorithm

The basic Kalman filter algorithm is used to obtain an improved estimation after the extended Kalman filter (EKF) algorithm has linearized the nonlinear state-space model and estimated the nonlinear system.[34, 35]. In addition to the Taylor series expansions of the state equation and the range equation, the partial derivatives of the observation equation and the state equation are also produced. The fundamentals of EKF and its use based on the battery's LSTM will be covered in this chapter. The classical EKF usually is divided into three parts, namely time update and measurement update, and its calculation procedure is shown in Equations.

The working steps of extended Kalman filtering:

Step 1: Calculate the state prediction and estimate the error covariance matrix as shown in Equations (12) and (13).

$$\hat{X}_{k+1/k} = A\hat{x}_k + Bu_k + v_1 \tag{12}$$

$$\tilde{P}_{k+1/k} = AP_k A_{k-1}^T + Q_{k-1} \tag{13}$$

Step 2: Calculate the Kalman gain K as shown in Equation (14).

$$K_k = \tilde{P}_{k+1/k} C^T (C\tilde{P}_{k+1/k} C^T + R_k)^{-1} \tag{14}$$

Step 3: Estimate system residual error, predict state and update the error covariance matrix as shown in Equation (15).

$$\begin{cases} \tilde{y}_{k+1} = y_{k+1} - (C\hat{x}_{k+1/k} + Du_{k+1}) + v_2 \\ \hat{x}_{k+1} = \hat{x}_{k+1/k} + K_k \tilde{y}_{k+1} \\ P_{k+1} = (I - K_k C)\tilde{P}_{k+1/k} \end{cases} \tag{15}$$

Where $x_k$is the system state at the sampling point k and $x^\wedge_k$ is its guess value; $P_k$is the covariance matrix of state error; x_0 is the initial system state and $x^\wedge_0$is its guess value; w_k is the process noise vector and Q_{k-1} are its covariance matrix; v_k is the measurement noise vector and $R_{k-1}$are its covariance matrix.

III. Experimental Analysis

3.1 Implementation of Test Platform

An experimental platform for lithium-ion batteries was constructed, and pertinent experiments were planned in accordance with the real working conditions to gather experimental data. This allowed for the verification of the model parameter's accuracy as well as the tracking of the filtered results of the SOC and the true values. Figure 2 displays the specifications of the lithium-ion batteries used in the experiment as well as the experimental apparatus.

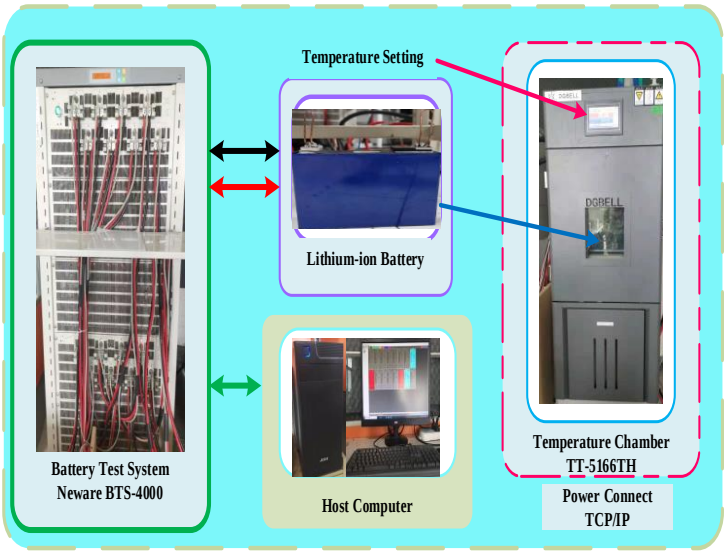

Parameters of Lithium-ion Battery	
Lithium-ion Battery Type	Ternary Lithium-ion Battery
Rated Capacity	40Ah
Nominal Voltage	3.7V
Maximum Sustained Discharge Rate	3C
Battery Weight	850g
Upper Charging Limit Voltage	4.2V
Lower Charging Limit Voltage	2.75

Figure 2: Experimental Set-up Equipment

A ternary lithium-ion battery with a 40Ah capacity and a 4.2V charging voltage is utilized in the experiment, as shown in Figure 2. Test box TT5166TT can regulate temperature by offering a consistent temperature during battery charging and discharging. When charging and discharging lithium-ion batteries, the Neware BTS-4000 battery test equipment is utilized as a high-power charge and discharge tester for power batteries.The process of charging and discharging The lithium-ion battery is linked to the charging and discharging method tester's host computer, which also configures the stages involved in the charging and discharging process. Such a main-machine interface module allows for control over the operating conditions of the lithium-ion battery experiment in a temperature-controlled environment.

3.2Complex Conditions

The voltage and current required for testing and training in the HPPC, BBDST, and DST operating environments. The battery is discharged to a cut-off voltage of 2.75V over the course of nine distinct charge-discharge cycles in the HPPC, BBDST, and DST operating conditions test. The changes in voltage and current that occur during HPPC, BBDST, and DST operations. Figure 3 displays the current and voltage for the training and testing profile under the BBDST, DST, and HPPC working conditions.

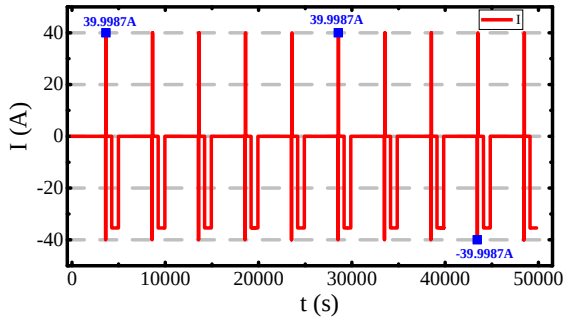

(a): Complete HPPC Current Curve

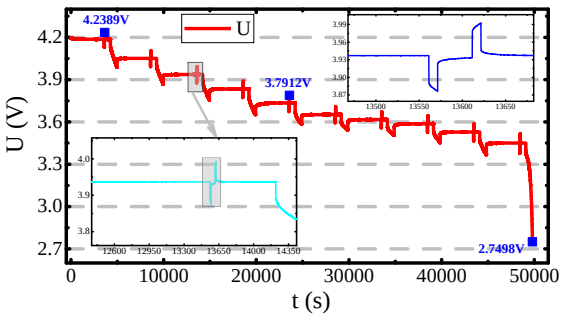

(b): Complete HPPC Voltage Curve

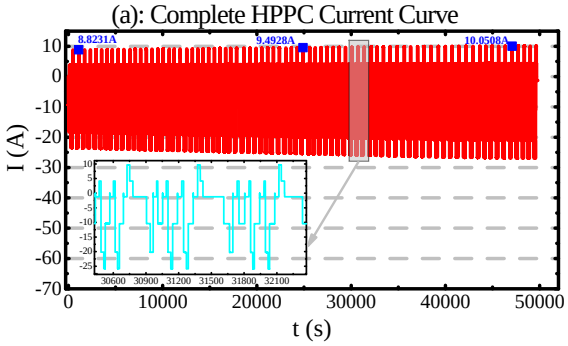

(c): Complete BBDST Current Curve

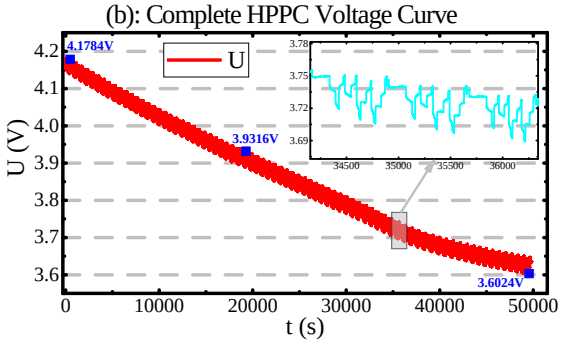

(d): Complete BBDST Voltage Curve

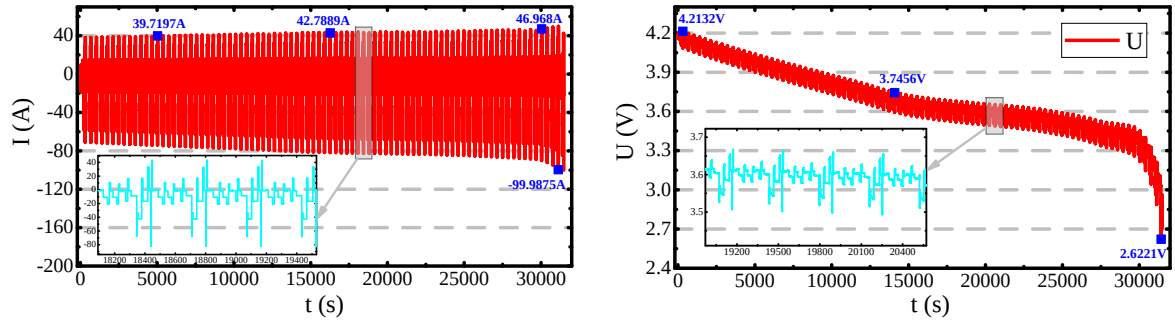

(e): Complete DST Current Curve (f): Complete DST Voltage Curve

Figure 3: The Training Current and Voltage Curves

Figure 3, contains the initial charging process. The acquired current and voltage data were internal resistance and SOC of the battery during the whole experiment was acquired. The final result of the state estimation is shown in Figure 4.

3.3Simulation and Verification of Algorithms

At a temperature of 25°C, the suggested LSTM-EKF is employed for SOC estimation and contrasted with LSTM under BBDST and HPPC operating circumstances. Figure 4 displays the SOC estimation outcomes for both techniques. The terminal voltage comparison utilized to update the state of charge estimation is this data. The LSTM-EKF technique uses the network to forecast and update the measured voltage under simulated noise and input the current.With an unknown initial value, the initial value of SOC is intentionally set to 1.0 to mimic interference in the estimating model. Figures 4(a), (b), and (d) display the algorithm's simulation results under HPPC conditions, and Figures 4(c), and (d) display the verification results under BBDST conditions. In these figures, the state ofcharge reference value is represented by the LSTM (SOC 1), the estimation result and error based on LSTM is represented by the (SOC 2), and the estimation result and error based on the LSTM-EKF network is represented by the error 1.

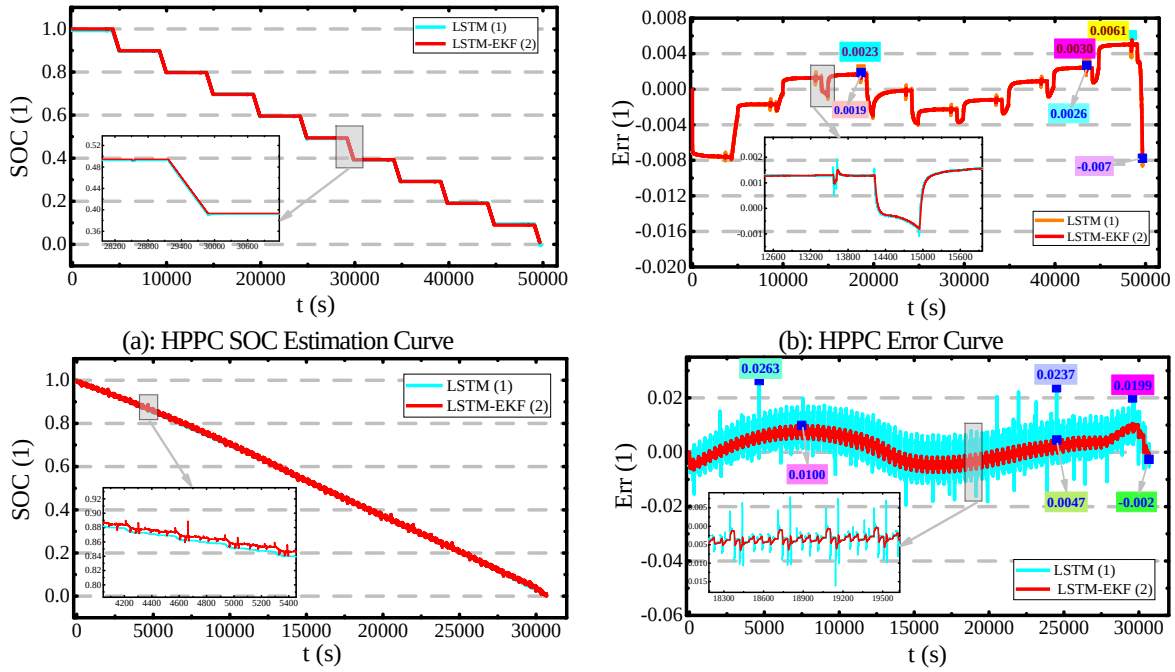

(a): HPPC SOC Estimation Curve (b): HPPC Error Curve

(c): BBDST SOC Estimation Curve (d): BBDST Error Curve

Figure 4: SOC Estimation Result Under HPPC and BBDST Working Conditions

Figure 4's estimation results show that, even in situations when the starting SOC value differs significantly from the real value, the method can nevertheless quickly converge to the true value under two different working conditions. By accounting for noise interference, the LSTM-EKF approach delivers higher estimation accuracy than the LSTM method. It is possible to deduce from the study of the output data that the LSTM-EKF model can detect noise and adapt itself automatically when the initial value is incorrect. The operating condition-based performance assessment of the LSTM and LSTM-EKF networks for the SOC

estimate.Due to the LSTM and LSTM-EKF model optimizer's infiltration, the model's results are not assessed under working conditions based on training methodology. These error results demonstrate the correctness and resilience of the suggested hybrid models, LSTM-EKF, in comparison to the data-driven approaches used in the model LSTM network. Both the estimation error result under the BBDST working condition and the maximum estimation error under the entire HPPC working condition are less than 0.03, indicating strong stability and robustness.

To assess the efficacy of the LSTM and LSTM-EKF models for the SOC estimation under HPPC and BBDST working circumstances, the error metrics are computed utilizing the identical training and testing sequence. The LSTM-EKF model is shown to have the fewest mistakes, and the network's errors rise in proportion to this. These error results demonstrate the correctness and resilience of the suggested hybrid models, LSTM-EKF, in comparison to the data-driven approaches used in the model LSTM network. Figure 5 shows the values of the MSE, MAE, and RMSE for the LSTM and LSTM-EKF models..

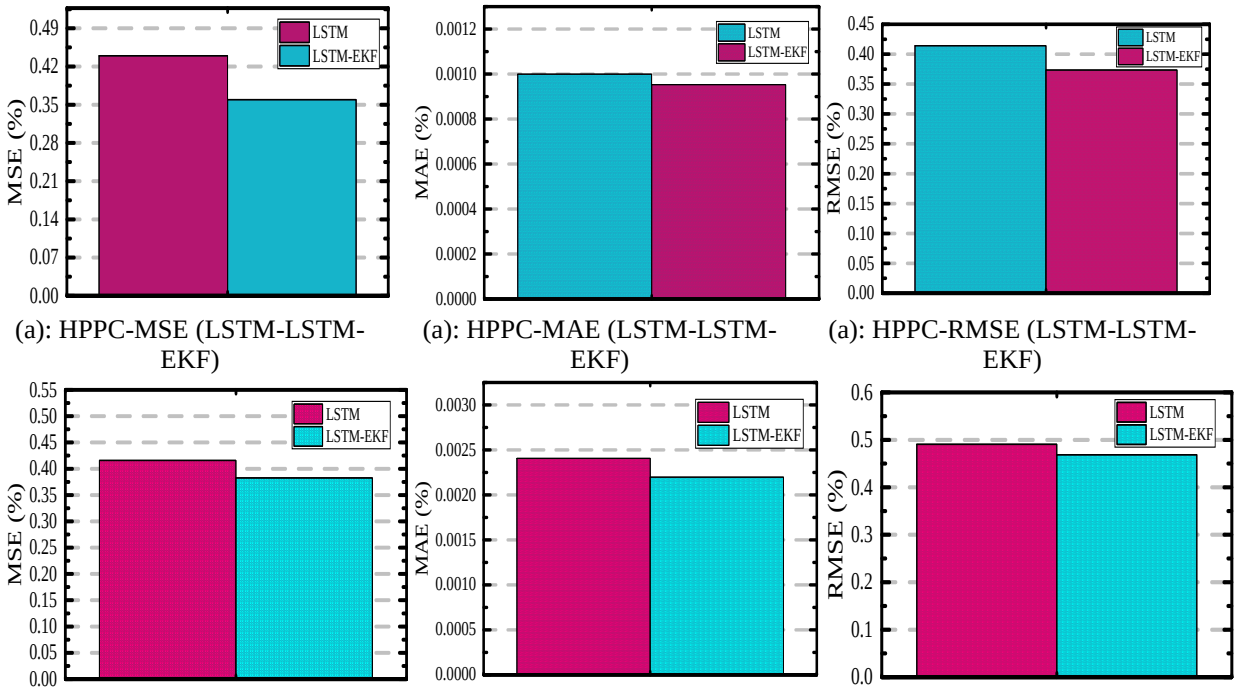

(a): HPPC-MSE (LSTM-LSTM-EKF) (a): HPPC-MAE (LSTM-LSTM-EKF) (a): HPPC-RMSE (LSTM-LSTM-EKF)

(b): BBDST-MSE (LSTM-LSTM-EKF) (b): BBDST-MAE (LSTM-LSTM-EKF) (b): BBDST-RMSE (LSTM-LSTM-EKF)

Figure 5:The Performance Analysis of the SOC Estimation Tested Under the HPPC and BBDST working conditions

The proposed hybrid models, LSTM-EKF, are more accurate and robust than data-driven LSTM network models when employing the identical training and testing sequence for SOC estimate, as demonstrated by these error results. The LSTM-EKF model serves as a reference for accuracy, and Table 1 displays the MSE, MAE, and RMSE values for the LSTM and LSTM-EKF models.

Table 1: Performance of LSTM and LSTM-EKF

Testing Working Conditions	**Error Metric**	**LSTM Network (%)**	**LSTM-EKF Network (%)**
	MSE	0.43967	0.35928
HPPC	MAE	9.99931E-4	9.53124E-4
	RMSE	0.41408	0.37355
	MSE	0.41584	0.38268
BBDST	MAE	0.00241	0.0022
	RMSE	0.49049	0.46877

A longitudinal comparison with the aforementioned table demonstrates that the two algorithms' convergence under the BBDST condition is superior to that under the HPPC condition. When compared to the LSTM network under the two conditions, the horizontal comparison demonstrates that the LSTM-EKF technique has certain advantages in terms of convergence. Because of the LSTM and LSTM-EKF models' optimizer infiltration, the results for these models are not assessed under the working condition-based training

technique.With the lowest MSE, MAE, and RMSE of 0.35928%, 9.53124%, and 0.37355%, respectively, under HPPC working conditions is the LSTM-EKF model. The lowest values of MSE, MAE, and RMSE for the BBDST operating condition are 0.38268%, 0.0022%, and 0.46877%, respectively. These findings demonstrate the adaptability, resilience, and competence of the suggested hybrid LSTM-EKF model for SOC estimation

IV. Conclusions

The research of the LSTM model network is utilized in the BBDST, DST, and HPPC working conditions for the SOC estimate of a lithium-ion battery based on a working condition training and testing datasets technique. The findings demonstrate how the working condition datasets used in training and testing affect the LSTM network's ability to estimate the SOC accurately. The LSTM's estimated SOC is fed into the EKF iteratively to improve the LSTM model's accuracy through denoising.The LSTM-EKF model, with the least MSE and improved robustness, has the best SOC estimate performance, the findings finally demonstrate. More rapidly and accurately than the LSTM model, it has better SOC initialization and adapts to the real SOC. To guarantee a steady-state estimate, it additionally denoised the predictions from the earlier models. It is found that the LSTM-EKF model outperforms the LSTM model in terms of convergence rate during the estimation process. This resolves the convergence and speed problems that are necessary for the SOC estimation to demonstrate its reliability, competency, and efficiency for an improved and logical real-time application of lithium-ion batteries.

Acknowledgments

The work is supported by the National Natural Science Foundation of China (No. 61801407), Sichuan Science and TechnologyProgram (No. 2019YFG0427), China Scholarship Council (No. 201908515099), and Fund of Robot Technology Used for Special Environment Key Laboratory of Sichuan Province (No. 18kftk03).

References

1. Gao, M., et al., Lithium metal batteries for high energy density: Fundamental electrochemistry and challenges. Journal of Energy Chemistry, 2021. **59**: p. 666-687.
[2]. Xu, J., et al., High-Energy Lithium-Ion Batteries: Recent Progress and a Promising Future in Applications. ENERGY & ENVIRONMENTAL MATERIALS, 2023. **6**(5): p. e12450.
[3]. Olabi, A.G., et al., Battery electric vehicles: Progress, power electronic converters, strength (S), weakness (W), opportunity (O), and threats (T). International Journal of Thermofluids, 2022. **16**: p. 100212.
[4]. Peng, J., et al., A comprehensive overview and comparison of parameter benchmark methods for lithium-ion battery application. Journal of Energy Storage, 2023. **71**: p. 108197.
[5]. Barzacchi, L., et al., Enabling early detection of lithium-ion battery degradation by linking electrochemical properties to equivalent circuit model parameters. Journal of Energy Storage, 2022. **50**: p. 104213.
[6]. Challoob, A.F., et al., Energy and battery management systems for electrical vehicles: A comprehensive review & recommendations. Energy Exploration & Exploitation, 2023. **42**(1): p. 341-372.
[7]. Zhang, Y. and Z. Hou, Battery Management System of Electric Vehicle, in Automated and Electric Vehicle: Design, Informatics and Sustainability, Y. Cao, Y. Zhang, and C. Gu, Editors. 2023, Springer Nature Singapore: Singapore. p. 23-44.
[8]. Manas, M., R. Yadav, and R.K. Dubey, Designing a battery Management system for electric vehicles: A congregated approach. Journal of Energy Storage, 2023. **74**: p. 109439.
[9]. Lakhotia, V.K. and R. Senthil Kumar, Review on various types of battery thermal management systems. Journal of Thermal Analysis and Calorimetry, 2023. **148**(22): p. 12335-12368.
[10]. See, K.W., et al., Critical review and functional safety of a battery management system for large-scale lithium-ion battery pack technologies. International Journal of Coal Science & Technology, 2022. **9**(1): p. 36.
[11]. Hannan, M.A., et al., Toward enhanced state of charge estimation of lithium-ion batteries using optimized machine learning techniques. Scientific reports, 2020. **10**(1): p. 1-15.
[12]. Zhang, X., et al. Study of SOC Estimation by the Ampere-Hour Integral Method with Capacity Correction Based on LSTM. Batteries, 2022. **8**, DOI: https://doi.org/10.3390/batteries8100170.
[13]. Wang, Q., et al., Transferable data-driven capacity estimation for lithium-ion batteries with deep learning: A case study from laboratory to field applications. Applied Energy, 2023. **350**: p. 121747.
[14]. Jiang, B., et al., An adaptive capacity estimation approach for lithium-ion battery using 10-min relaxation voltage within high state of charge range. Energy, 2023. **263**: p. 125802.
[15]. Baduge, S.K., et al., Artificial intelligence and smart vision for building and construction 4.0: Machine and deep learning methods and applications. Automation in Construction, 2022. **141**: p. 104440.
[16]. Taye, M.M. Understanding of Machine Learning with Deep Learning: Architectures, Workflow, Applications and Future Directions. Computers, 2023. **12**, DOI: 10.3390/computers12050091.
[17]. Zhou, W., et al. Review on the Battery Model and SOC Estimation Method. Processes, 2021. **9**, DOI: 10.3390/pr9091685.
[18]. Matviychuk, Y., et al., Improving the accuracy of model-based quantitative nuclear magnetic resonance. Magn. Reson., 2020. **1**(2): p. 141-153.
[19]. Rios, J., An Examination of Individual Ability Estimation and Classification Accuracy Under Rapid Guessing Misidentifications. Applied Measurement in Education, 2022. **35**(4): p. 300-312.
[20]. Dini, P., A. Colicelli, and S. Saponara Review on Modeling and SOC/SOH Estimation of Batteries for Automotive Applications. Batteries, 2024. **10**, DOI: 10.3390/batteries10010034.
[21]. Aldoseri, A., K.N. Al-Khalifa, and A.M. Hamouda Re-Thinking Data Strategy and Integration for Artificial Intelligence: Concepts, Opportunities, and Challenges. Applied Sciences, 2023. **13**, DOI: 10.3390/app13127082.

[22]. Chandran, V., et al. State of Charge Estimation of Lithium-Ion Battery for Electric Vehicles Using Machine Learning Algorithms. World Electric Vehicle Journal, 2021. **12**, DOI: 10.3390/wevj12010038.
[23]. Wang, H.K., Y. Zhang, and M. Huang, A conditional random field based feature learning framework for battery capacity prediction. Sci Rep, 2022. **12**(1): p. 13221.
[24]. Chen, K., et al., State of charge estimation for lithium-ion battery based on whale optimization algorithm and multi-kernel relevance vector machine. J Chem Phys, 2023. **158**(10): p. 104110.
[25]. Liu, B., et al., Immovable Cultural Relics Disease Prediction Based on Relevance Vector Machine. Mathematical Problems in Engineering, 2020. **2020**: p. 9369781.
[26]. Deringer, V.L., et al., Gaussian Process Regression for Materials and Molecules. Chemical Reviews, 2021. **121**(16): p. 10073-10141.
[27]. Zhao, S., L. Chen, and Y. Huang ADAS Simulation Result Dataset Processing Based on Improved BP Neural Network. Data, 2024. **9**, DOI: 10.3390/data9010011.
[28]. Teixeira, R.S.D., et al. Recurrent Neural Networks for Estimating the State of Health of Lithium-Ion Batteries. Batteries, 2024. **10**, DOI: 10.3390/batteries10030111.
[29]. Hussein, H.M., et al. Comparative Study-Based Data-Driven Models for Lithium-Ion Battery State-of-Charge Estimation. Batteries, 2024. **10**, DOI: 10.3390/batteries10030089.
[30]. Xu, P., et al., State of health estimation of LIB based on discharge section with multi-model combined. Heliyon, 2024. **10**(4): p. e25808.
[31]. Yao, L., et al. State of Health Estimation Based on the Long Short-Term Memory Network Using Incremental Capacity and Transfer Learning. Sensors, 2022. **22**, DOI: 10.3390/s22207835.
[32]. Zhang, L., et al. Accurate Prediction Approach of SOH for Lithium-Ion Batteries Based on LSTM Method. Batteries, 2023. **9**, DOI: 10.3390/batteries9030177.
[33]. Gu, B. and Z. Liu Transfer Learning-Based Remaining Useful Life Prediction Method for Lithium-Ion Batteries Considering Individual Differences. Applied Sciences, 2024. **14**, DOI: 10.3390/app14020698.
[34]. Di_çi, F.N., Y. El-Kahlout, and A. Balikci, Li-ion battery modeling and SOC estimation using extended Kalman filter. 2017 10th International Conference on Electrical and Electronics Engineering (ELECO), 2017: p. 166-169.
[35]. Yang, S., et al., A parameter adaptive method for state of charge estimation of lithium-ion batteries with an improved extended Kalman filter. Scientific Reports, 2021. **11**(1): p. 5805.